Stochastic-Constraints Method in Nonstationary Hot-Clutter Cancellation — Part I: Fundamentals and Supervised Training Applications

Prof. Yuri I. Abramovich [1,2]

[1] Surveillance Systems Division, Defence Science and Technology Organisation (DSTO)
PO Box 1500, Edinburgh S.A. 5111, Australia

[2] Cooperative Research Centre for Sensor Signal and Information Processing (CSSIP)
SPRI Building, Technology Park Adelaide, Mawson Lakes S.A. 5095, Australia

yuri@cssip.edu.au

Abstract

We consider the use of spatio-temporal adaptive array processing in over-the-horizon radar applications in order to remove nonstationary multipath interference, known as "hot clutter". Since the spatio-temporal properties of hot clutter cannot be assumed constant over the coherent processing interval, conventional adaptive techniques fail to provide effective hot-clutter mitigation without simultaneously degrading the properties of the backscattered radar signals, known as "cold clutter". The approach presented incorporates multiple "stochastic" (data-dependent) constraints to achieve effective hot-clutter suppression, whilst maintaining distortionless output cold-clutter post-processing stationarity.

1. Introduction

This lecture is concerned with adaptive processing of data from high frequency (HF) over-the-horizon radar (OTHR). In general, such radar systems operate by collecting data over a coherent processing interval of time (CPI) which consists of N transmitted pulses or sweeps (in the case of continuous wave (CW) radars), emitted at a pulse repetition frequency of f_r pulses per second. The receiving system consists of M elements, subarrays for example, with each element linked to an individual digital receiver. Receiver outputs are sampled at the Nyquist rate of f_t samples per second, resulting in T samples per pulse repetition interval (PRI). The total set of data collected in this manner during a single CPI therefore consists of $M \times N \times T$ samples. Increments in the Nyquist rate (range bins) within a particular PRI are called *fast-time* samples, while those across PRIs are termed *slow-time* samples.

For typical sky-wave OTHR, we have $M = 16$ to 32, $N = 128$ to 256 and $T \simeq 50$ to 60 [1]; while for surface-wave radars, the CPI may approach 60 or 120 sec [2], so that even with $f_t = 10$ Hz, we have $N = 1000$.

For HF OTHR, an interference signal produced by a single source is typically seen as a multiplicity of interference signals at the receiving antenna array, each mode propagating from source to receiver along a different path.

Various ionospheric layers and inhomogeneities involved in the reflection of interference signals are responsible for the so-called *hot-clutter* phenomenon. If the propagation paths involve reflections from highly perturbed and nonstationary ionospheric regions (such as the equatorial "hot plasma" area or the polar regions), then for hot clutter, nonstationarity of the spatio-temporal covariance matrix over a typical CPI is inevitable. Indeed, spatial nonstationarity of ionospherically propagated interference signals has been observed in HF OTHR, even over the relatively short CPIs typical for aircraft detection [3]. Consideration of this phenomenon is found to be essential for ship detection via skywave propagation, and even more so for HF surface-wave radars where nonstationarity over much longer CPIs leads to a dramatic degradation in the performance of most existing adaptive interference cancellation techniques [3].

It is important to note the critical distinction between hot clutter and ordinary *cold clutter*: the latter is a reflection of the radiated radar signal, while the former refers to the (diffuse) multipath scattered jammer signals.

Paper presented at the RTO SET Lecture Series on "Military Application of Space-Time Adaptive Processing", held in Istanbul, Turkey, 16-17 September 2002; Wachtberg, Germany, 19-20 September 2002; Moscow, Russia, 23-24 September 2002, and published in RTO-EN-027.

Of course, the so-called "general fully adaptive" spatio-temporal processing (STAP) described in [4] for example, can theoretically solve the problem of joint hot and cold-clutter suppression [5]. However, in practice this is rarely possible because the dimension of such a fully adaptive system would be MNQ, where Q is the number of fast-time samples involved (number of taps). Indeed, for any HF application with $N \gtrsim 128$, a fully adaptive scheme is totally impractical simply due to the lack of, say, $2MNQ$ training samples.

Thus from a practical viewpoint, we should consider a scheme whereby each "finger beam" is associated with an MQ-variate fast-time STAP to reject the (diffuse) jammer multipath (hot clutter). For HF OTHR applications, the output signals of each beam should be processed by the standard slow-time inter-PRI coherent processing (Doppler spectrum analysis), provided that the cold-clutter slow-time properties at the scalar finger-beam output are not perturbed by the previous fast-time STAP.

Obviously for sufficiently high nonstationarity of the hot-clutter signal, this is a problem since the uncontrolled pattern fluctuations over the CPI introduced by conventional fast-time STAP modulate and consequently decorrelate the cold-clutter signal. For purely spatial adaptive processing, this latter phenomenon has been established both theoretically and experimentally in HF OTHR [6, 3, 7, 8].

Note that if the cold-clutter signal was created by a limited number of point scatterers, it would be possible to "freeze" the receiving antenna pattern in the direction of each point scatterer using standard linear deterministic constraints [9], which are normally used in order to "protect" the antenna pattern in the expected signal direction. Clearly the spatial distribution of cold clutter is generally quite broad, so that it is collected by most of the antenna beam-pattern rather than in just a few directions. Therefore the above method is inappropriate, since we are not able to "freeze" the entire pattern or even a significant part of it without a dramatic degradation in hot clutter rejectability.

Another quite straight-forward approach in avoiding antenna fluctuations is to return to the time-invariant (over CPI) fast-time STAP. The technique of averaging the nonstationary covariance matrix over the CPI has been introduced and tested for HF OTHR applications [6, 3], where it was demonstrated that this approach is appropriate only for extremely short CPIs. The paper [3] defines the typical "stationarity interval" for ionospherically propagated jammers within the dynamic range of contemporary digital receivers to be 100 to 150 μsec, which includes only a few PRIs. Jammer averaging over this interval usually leads to the acceptable degradation of 1 to 3 dB in jamming rejectability compared with "quasi-instantaneous" covariance matrix estimation which uses fast-time training samples in the immediate neighborhood of the analyzed samples within the same PRI, where the delay between the training samples and the operational ranges can be ignored.

Therefore for HF OTHR ($N = 128$), this approach is also completely inappropriate, though the property of "local stationarity" over the short interval of a few consecutive repetition periods will be heavily exploited in what follows.

To summarize, no existing technique is able to provide over sufficiently long CPIs a highly effective hot-clutter-only mitigation without compromising the cold-clutter processing. The main objective of this lecture is to introduce an approach whereby the nonstationary hot-clutter rejection is performed by fast-time STAP updated from PRI to PRI, while the slow-time correlation properties of the cold-clutter scalar output are not affected by the STAP temporal fluctuations.

A spatial-only adaptive processing (SAP) technique involving stochastic constraints was recently introduced to solve this problem [6, 3, 7, 8]. This technique was experimentally verified for HF OTHR, with results reported in [3, 8]. Here we refer to the generalization of this the stochastic-constraints approach to spatio-temporal adaptive rejection of hot clutter which is essentially nonstationary over the CPI [15].

2. SC STAP Algorithm: Model Description

Let the M-variate complex column vector $\boldsymbol{z}_{kt}$ be the antenna array snapshot corresponding to the k^{th} repetition period and the t^{th} range bin, *ie.* $\boldsymbol{z}_{kt} \in \mathcal{C}^{M\times 1}$ where k represents "slow time" while t represents "fast time". In general, we may define the snapshot $\boldsymbol{z}_{kt}$ to be the mixture

$$\boldsymbol{z}_{kt} = \boldsymbol{s}_{kt} + \boldsymbol{y}_{kt} + \boldsymbol{x}_{kt} + \boldsymbol{\eta}_{kt} \qquad \text{for} \quad k =,1\ 2, \ldots, N; \quad t =,1\ 2, \ldots, T \tag{1}$$

where $\boldsymbol{s}_{kt}$ is the desired signal backscattered by a point target; $\boldsymbol{y}_{kt}$ is the radar signal backscattered by terrain or the sea surface ("cold clutter"); $\boldsymbol{x}_{kt}$ is the total jamming signal, comprising direct path, specular and diffuse multipath scattering ("hot clutter"); and $\boldsymbol{\eta}_{kt}$ is additive white noise of power $\sigma_{\boldsymbol{\eta}}^2$ with the correlation property

$$\mathcal{E}\{\boldsymbol{\eta}_{kt}\ \boldsymbol{\eta}_{k't'}^H\} = \sigma_{\boldsymbol{\eta}}^2\,\delta(k-k')\,\delta(t-t')\,I_M\,. \tag{2}$$

Typically, the target signal $\boldsymbol{s}_{kt}$ originating from some direction θ_0 takes the form

$$\boldsymbol{s}_{kt} = a\,\psi_t\,\exp\Big(i\,[\omega_d\,k/f_r + \phi_t]\Big)\,\boldsymbol{s}(\theta_0) \tag{3}$$

where a is a complex Gaussian-distributed (scalar) amplitude; ψ_t is the signal waveform; ω_d is the target-signal Doppler frequency (in radians); ϕ_t is a range-dependent phase, and $\boldsymbol{s}(\theta_0)$ is the array manifold ("steering") vector.

The cold-clutter snapshot $\boldsymbol{y}_{kt}$ is simulated here as a stationary random M-variate Gaussian process with the correlation property

$$\mathcal{E}\{\boldsymbol{y}_{kt}\ \boldsymbol{y}_{k't'}^H\} = \delta(t-t')\,R_{k-k'}^{\boldsymbol{y}} \tag{4}$$

(*ie.* the range sidelobes are ignored) where $R_{k-k'}^{\boldsymbol{y}}$ is the cold-clutter spatial covariance matrix at the slow-time lag $(k-k')$, and $R_0^{\boldsymbol{y}}$ is the standard M-variate Hermitian cold-clutter spatial covariance matrix.

The hot-clutter signal $\boldsymbol{x}_{kt}$ is assumed to be a convolutive mixture of P external interference signals $g_{kt}^{(p)}$, $p = 1, \ldots, P$, where each $g_{kt}^{(p)}$ is a complex waveform radiated by the p^{th} jammer at time $(k/f_r + t)$:

$$\boldsymbol{x}_{kt} = \sum_{\ell=1}^{L} H_{k\ell}\,\boldsymbol{g}_{k,t-\ell+1} \tag{5}$$

where L is the assumed maximum number of propagating paths for any of the P interfering sources, and $H_{k\ell}$ is defined below. The P-variate vector $\boldsymbol{g}_{kt} = \left[g_{kt}^{(1)}, \ldots, g_{kt}^{(P)}\right]^T$ consists of complex waveforms radiated by all P sources at time $(k/f_r + t)$.

As usual, we assume that

$$\mathcal{E}\left\{g_{kt}^{(p)}\,g_{k't'}^{(p')*}\right\} = \delta(p-p')\,\delta(k-k')\,\delta(t-t')\,\sigma_{\boldsymbol{x}_p}^2 \tag{6}$$

where $\sigma_{\boldsymbol{x}_p}^2$ is the p^{th} jamming signal power, *ie.* the jammers are assumed to be mutually independent and temporally white (broadband).

For diffuse multipath, L is usually defined as the number of range bins covering some range interval Δ_R involved in the scattering [9, 4]—

$$L = \frac{B\Delta_R}{c} = f_t\Delta_R \tag{7}$$

where B is the signal bandwidth, and c is the speed of light. For continuously distributed scatterers, it is more accurate to determine the interval between lines of constant path delay by the range grid, defined by the maximum hot-clutter suppression for continuously distributed clutter. The latter itself is usually defined by the input hot-clutter-to-noise ratio. The larger this ratio is, the smaller the separation should be. This phenomenon has been known for many years [10, 11]; an example of the accurate evaluation of the number L is given in [4] for one particular hot-clutter-to-noise ratio.

The MP-variate matrix $H_{k\ell}$ introduced above in (5) represents the instantaneous total impulse response, relating the radiated jammer signals $g_{kt}^{(p)}$ to the received hot-clutter snapshots $\boldsymbol{x}_{kt}$. Naturally $H_{k\ell}$ incorporates the time-varying channel characteristics experienced by each propagation path. For diffuse multipath, the time variation of the synthetic wavefront from the scatterers along each line of constant path delay is defined by a differential Doppler shift along that line. More precisely, the $(i,j)^{th}$ element of the matrix $H_{k\ell}$ is a complex

coefficient which is practically constant over the k^{th} PRI, and is a measure of the contribution of the j^{th} interference source with relative delay ℓ to the final hot-clutter output at the i^{th} receiver during the k^{th} PRI.

Although the number of interfering sources P is assumed to be strictly less than the number of antenna elements M, the total number of independent sources seen by the antenna array may approach PL. Thus, even for modest P and L, their product may exceed the number of antenna elements M. If

$$PL \geq M \tag{8}$$

then a purely spatial approach will be generally ineffective. On the other hand, it is necessary to emphasize that the product PL itself does not entirely define the best performance of the adaptive technique. For example, if all scatterers are situated in an extremely thin layer (of the ionosphere) with constant path delay ("auroral" scattering), then the rank of the covariance matrix would always be unity for a single jamming source. Therefore in this case, pure SAP would give us the maximum efficiency for distributed scattering cancellation, regardless of the number of such point scatterers. This phenomenon was described in [11].

Equally, pure SAP should deliver effective hot-clutter cancellation for a single jammer if

$$L \ll M\,. \tag{9}$$

The existence of numerous point scatterers along the path of equal delay over a wide angle means that the main beam direction will be unaffected by SAP, even if this main beam intersects this path [11, 4]. On the other hand, if there is a single scatterer along the path of equal delay which intersects the main beam, then pure SAP would not deliver effective suppression of hot clutter collected by the main beam. To be more accurate, under the condition $L \ll M$, such hot clutter could be rejected, but the main beam would also be affected.

These quite simple considerations are necessary for a clear understanding of the correspondence between SAP and STAP in the hot-clutter mitigation problem.

Hereafter we will be dealing with the general case $PL \geq M$.

If the model of (5) is adopted for some fixed L, then we note that the number of taps Q that are necessary for hot-clutter suppression is defined directly by the model. Let us introduce the MQ-variate "stacked" vector $\tilde{\boldsymbol{x}}_{kt}$, consisting of Q successive fast-time samples $\boldsymbol{x}_{kt}$ stacked on top of each other. According to (5), we may write

$$\begin{bmatrix} \boldsymbol{x}_{kt} \\ \boldsymbol{x}_{k,t-1} \\ \vdots \\ \boldsymbol{x}_{k,t-Q+1} \end{bmatrix} = \begin{bmatrix} H_{k0} & \dots & H_{k,L-1} & 0 & \dots & 0 \\ 0 & H_{k0} & \dots & H_{k,L-1} & \ddots & \vdots \\ \vdots & \ddots & \ddots & & \ddots & 0 \\ 0 & \dots & 0 & H_{k0} & \dots & H_{k,L-1} \end{bmatrix} \begin{bmatrix} \boldsymbol{g}_{kt} \\ \boldsymbol{g}_{k,t-1} \\ \vdots \\ \boldsymbol{g}_{k,t-L+1-Q+1} \end{bmatrix} \tag{10}$$

or more compactly

$$\tilde{\boldsymbol{x}}_{kt} = \tilde{H}_{k\ell}\, \tilde{\boldsymbol{g}}_{kt}\,. \tag{11}$$

The number of rows in the stacked block matrix $\tilde{H}_{k\ell}$ is equal to MQ, while the number of columns is $P(L+Q-1)$. Thus the stacked noise-free hot-clutter spatio-temporal covariance matrix

$$\tilde{R}_k^{\boldsymbol{x}} = \mathcal{E}\{\tilde{\boldsymbol{x}}_{kt}\, \tilde{\boldsymbol{x}}_{kt}^H\} \tag{12}$$

is always rank-deficient if

$$MQ > P(L+Q-1) \tag{13}$$

ie.

$$Q > \frac{P(L-1)}{M-P}\,. \tag{14}$$

This condition and the basic presentation of (10) are well known in the field of multiple-input-multiple-output (MIMO) systems [12].

For $L = 1$, STAP cannot outperform SAP, as expected. While for $Q = 1$, we find that the covariance matrix is rank-deficient if $M > PL$, *ie.* SAP alone can effectively suppress hot clutter.

It is interesting to note that the number of taps $Q = L$ usually recommended [9, 4] is justified only for $P = M/2$. The number of taps necessary to cope with the maximum number of independent jammers $P_{max} = M-1$ is

$$Q_{max} \geq P_{max}\,(L-1) \tag{15}$$

which again agrees with the results of MIMO studies [12].

Note that when the condition of (13) is satisfied, the rank of the covariance matrix $\tilde{R}_k^{\boldsymbol{x}}$ is

$$\text{rank}\,[\tilde{R}_k^{\boldsymbol{x}}] \lesssim P(L+Q-1)\,. \tag{16}$$

Thus the condition (13) actually generalizes the well-known condition for spatial suppression of P independent jammers

$$M > P \tag{17}$$

which obviously follows from (13) when $Q = L = 1$.

It is necessary to emphasize that the condition of (13) or (17) guarantees hot-clutter rejectability irrespective of the signal-to-noise ratio (SNR) obtained as a result of such rejection. For independent jammers and pure SAP, the main beam would be affected when the direction of arrival of one of the jammers is close to the target signal direction. For STAP a similar unfortunate scenario may occur, when the target-signal stacked vector $\tilde{\boldsymbol{s}}_{kt}$ (defined similarly to $\tilde{\boldsymbol{x}}_{kt}$ and $\tilde{\boldsymbol{g}}_{kt}$) can be fairly accurately presented as a linear combination of the columns of $\tilde{H}_{k\ell}$.

Obviously, in practical applications, Q should exceed Q_{min} as defined by (14) because of the additional constraints that are usually imposed.

Suppose now that the number of taps Q is properly chosen, and so our problem is to find an MQ-variate STAP filter $\tilde{\boldsymbol{w}}_{kt}$ with which to process the MQ-variate stacked vector $\tilde{\boldsymbol{z}}_{kt}$:

$$\tilde{\boldsymbol{z}}_{kt} = \begin{bmatrix} \boldsymbol{z}_{kt} \\ \vdots \\ \boldsymbol{z}_{k,t-Q+1} \end{bmatrix} \tag{18}$$

to form the scalar output $z_{kt} = \tilde{\boldsymbol{w}}_{kt}^H\,\tilde{\boldsymbol{z}}_{kt}$. We may similarly compute the scalar output sequences which correspond to the target signal $\boldsymbol{s}_{kt}$, the backscattered cold clutter $\boldsymbol{y}_{kt}$, and the hot clutter $\boldsymbol{x}_{kt}$:

$$\begin{aligned} s_{kt} &= \tilde{\boldsymbol{w}}_{kt}^H\,\tilde{\boldsymbol{s}}_{kt} \\ y_{kt} &= \tilde{\boldsymbol{w}}_{kt}^H\,\tilde{\boldsymbol{y}}_{kt} \\ x_{kt} &= \tilde{\boldsymbol{w}}_{kt}^H\,\tilde{\boldsymbol{x}}_{kt}\,. \end{aligned} \tag{19}$$

The first set of constraints for the STAP vector $\tilde{\boldsymbol{w}}_{kt}$ is designed to ensure the undistorted reception of the target signal. There are several approaches using deterministic linear constraints which can protect the desired signal against distortions caused by temporal adaptivity [9]. For example, we may introduce the set of Q linear constraints such that

$$\tilde{\boldsymbol{w}}_{kt}^H\,A_Q(\theta_0) = \boldsymbol{e}_Q^T \tag{20}$$

where the $MQ \times Q$ matrix $A_Q(\theta_0) = \boldsymbol{s}(\theta_0) \otimes I_Q$ ($\otimes$ represents the Kronecker product) and the Q-variate column vector $\boldsymbol{e}_Q = [1, 0, \ldots, 0]^T$.

Such constraints ensure the distortionless reception of the target signal from the expected DOA θ_0. If one requires the output signal s_{kt} to be more robust in the presence of pointing errors, constraints on the steering vector derivatives might also be imposed, *eg.*

$$A_{2Q}(\theta_0) = \begin{bmatrix} \boldsymbol{s}(\theta_0) & \boldsymbol{s}'(\theta_0) & 0 & 0 & \ldots & 0 & 0 \\ 0 & 0 & \boldsymbol{s}(\theta_0) & \boldsymbol{s}'(\theta_0) & & 0 & 0 \\ \vdots & & & & \ddots & & \vdots \\ 0 & 0 & \ldots & 0 & 0 & \boldsymbol{s}(\theta_0) & \boldsymbol{s}'(\theta_0) \end{bmatrix} \tag{21}$$

where

$$s'(\theta_0) = \left.\frac{\partial s(\theta)}{\partial \theta}\right|_{\theta=\theta_0} \tag{22}$$

and

$$\tilde{w}_{kt}^H A_{2Q}(\theta_0) = e_{2Q}^T . \tag{23}$$

In general, we may define an $MQ \times q$ matrix $\tilde{A}_q$ together with the q-variate vector e_q to implement q linear constraints:

$$\tilde{w}_{kt}^H \tilde{A}_q(\theta_0) = e_q^T . \tag{24}$$

The cold clutter is assumed to be a stationary process (in a broad sense), and thus it may be approximated by the multivariate auto-regressive (AR) model of order κ:

$$y_{kt} + \sum_{j=1}^{\kappa} B_j\, y_{k-j,t} = \xi_{kt} . \tag{25}$$

In the above equation, B_j are the M-variate matrices which are the solutions of the multivariate Yule-Walker equations [13]:

$$\begin{bmatrix} R_0^y & R_1^y & \dots & R_\kappa^y \\ R_{-1}^y & R_0^y & & \\ \vdots & & \ddots & \vdots \\ R_{-\kappa}^y & & \dots & R_0^y \end{bmatrix} \begin{bmatrix} I_M \\ B_1 \\ \vdots \\ B_\kappa \end{bmatrix} = \begin{bmatrix} R_k^\xi \\ 0 \\ \vdots \\ 0 \end{bmatrix} \tag{26}$$

where

$$\mathcal{E}\{\xi_{kt}\, \xi_{k+j,t}^H\} = \begin{cases} R_k^\xi & \text{for } j = 0 \\ 0 & \text{for } j \neq 0 . \end{cases} \tag{27}$$

Note that the scalar moving average (MA) model is usually considered an alternative to the AR model, however it is now known that even the multivariate MA model can be presented as a multivariate AR model of finite order under surprisingly mild conditions [14] (in the scalar case this order is infinite).

In [15], we derived for this general model the exact analytic solution for a time-varying fast-time STAP filter that maintains the stationarity of the cold-clutter scalar output signal, regardless of the filter's temporal fluctuations. Yet, practically feasible solutions, demonstrated below, may be derived for the simpler scalar multivariate model:

$$y_{kt} + \sum_{j=1}^{\kappa} b_j\, y_{k-j,t} = \xi_{kt} \tag{28}$$

where $B_j = b_j\, I_m$.

3. SC STAP Algorithm: Practical Routine for Pulse-Waveform (PW) HF OTHR

An operational (practical) approach for purely spatial adaptive processing was introduced in [6, 3, 7, 8]; we shall now generalize this to the STAP case.

In most PW HF OTHR systems, scattering from the Earth's surface (cold clutter) and from targets occupies only a limited range within each repetition period. For sky-wave radar, the finite duration of the oblique backscattered signal (OBS) is dictated by the radar–ionosphere–target geometry. For surface-wave radar, natural attenuation leads to suppression of the backscattered signal far from the end of the repetition period. Naturally these scattered (cold-clutter) signals are submerged in the hot clutter and are not directly available for treatment by stochastic constraints.

Meanwhile, the hot-clutter signal usually occupies the entire repetition period (the entire CPI, actually) and in most cases some region within the PRI can be easily identified as containing hot clutter only. Hence this

operational routine relies on *a priori* information on the distribution of the cold-clutter-free ranges within the PRI.

We have already discussed the "local stationarity" property of the hot clutter over the limited number of consecutive PRIs. Assume for example, the second-order ($\kappa = 2$) cold-clutter AR model of the simple scalar multivariate model (28). We form the fast-time STAP filters $\tilde{\boldsymbol{w}}_{kt}^{av}$ in the order $k = 1, \ldots, N-\kappa$; the first of which ($k = 1$) is stochastically unconstrained, and thereafter are stochastically constrained. We construct this initial STAP filter $\tilde{\boldsymbol{w}}_{1t}^{av}$ using the hot-clutter-only training samples from some common range region within the first three consecutive PRIs:

$$\tilde{\boldsymbol{w}}_{1t}^{av} = \left(\tilde{R}_1^{av}\right)^{-1} \tilde{A}_q(\theta_0) \left[\tilde{A}_q^H(\theta_0) \left(\tilde{R}_1^{av}\right)^{-1} \tilde{A}_q(\theta_0)\right]^{-1} \boldsymbol{e}_q \tag{29}$$

where $\tilde{A}_q(\theta_0)$ and $\boldsymbol{e}_q$ are the deterministic constraints from (24) and

$$\tilde{R}_1^{av} = \frac{1}{3}\left(\tilde{R}_1^{\boldsymbol{x}\boldsymbol{\eta}} + \tilde{R}_2^{\boldsymbol{x}\boldsymbol{\eta}} + \tilde{R}_3^{\boldsymbol{x}\boldsymbol{\eta}}\right). \tag{30}$$

Due to the "local stationarity" of the hot clutter, we believe that the hot-clutter samples are properly rejected by the STAP filter $\tilde{\boldsymbol{w}}_{1t}^{av}$ over all ranges of these three initial PRIs, so that the scalar output for operational ranges consists mainly of cold clutter, noise and possible targets, *ie.*

$$\tilde{\boldsymbol{w}}_{1t}^{avH}\, \tilde{\boldsymbol{z}}_{kt} \simeq \tilde{\boldsymbol{w}}_{1t}^{avH}\, \tilde{\boldsymbol{y}}_{kt} + \tilde{\boldsymbol{w}}_{1t}^{avH}\, \tilde{\boldsymbol{s}}_{kt} + \tilde{\boldsymbol{w}}_{1t}^{avH}\, \tilde{\boldsymbol{\eta}}_{kt} \qquad \text{for} \quad k = 1, 2, 3. \tag{31}$$

Note that $\tilde{\boldsymbol{w}}_{1t}^{av}$ is a function only of k, not of fast time t. For the next adaptive filter $\tilde{\boldsymbol{w}}_{2t}^{av}$ (now range-dependent and stochastically constrained), we apply the "sliding-window" average to the next three repetition periods:

$$\tilde{R}_2^{av} = \frac{1}{3}\left(\tilde{R}_2^{\boldsymbol{x}\boldsymbol{\eta}} + \tilde{R}_3^{\boldsymbol{x}\boldsymbol{\eta}} + \tilde{R}_4^{\boldsymbol{x}\boldsymbol{\eta}}\right) \tag{32}$$

to again ensure a proper hot-clutter suppression over these three PRIs. Clearly the moving-average across $(\kappa+1)$ adjacent repetition periods also ensures that κ covariances $\tilde{R}_k^{\boldsymbol{x}\boldsymbol{\eta}}$ are common to each successive average $\tilde{R}_k^{av}$. The system of κ stochastic constraints corresponding to (31) and (32) may then be written as:

$$\tilde{\boldsymbol{w}}_{2t}^{avH}\, \tilde{\boldsymbol{z}}_{kt} = \tilde{\boldsymbol{w}}_{1t}^{avH}\, \tilde{\boldsymbol{z}}_{kt} \qquad \text{for} \quad k = 2, 3. \tag{33}$$

The right-hand sides of these constraints consist of the cold-clutter samples mainly due to (31); whereas (32) ensures that the filter $\tilde{\boldsymbol{w}}_{2t}^{av}$ properly processes the cold-clutter samples only, since the hot-clutter component is to be rejected.

For an arbitrary slow time k, the operational solution

$$\tilde{\boldsymbol{w}}_{kt}^{av} = \left(\tilde{R}_k^{av}\right)^{-1} \tilde{A}_{kt}^{\boldsymbol{z}} \left[\tilde{A}_{kt}^{\boldsymbol{z}H} \left(\tilde{R}_k^{av}\right)^{-1} \tilde{A}_{kt}^{\boldsymbol{z}}\right]^{-1} \boldsymbol{e}_{q+\kappa} \qquad \text{for} \quad k = 2, \ldots, N-2 \tag{34}$$

is defined by the "sliding-window" covariance matrix

$$\tilde{R}_k^{av} = \frac{1}{3}\left(\tilde{R}_k^{\boldsymbol{x}\boldsymbol{\eta}} + \tilde{R}_{k+1}^{\boldsymbol{x}\boldsymbol{\eta}} + \tilde{R}_{k+2}^{\boldsymbol{x}\boldsymbol{\eta}}\right) \tag{35}$$

and the system of stochastic constraints

$$\tilde{A}_{kt}^{\boldsymbol{z}} = \left[\tilde{A}_q \,\middle|\, \left(\tilde{I}_{MQ} - \frac{\tilde{\boldsymbol{s}}(\theta_0)\, \tilde{\boldsymbol{w}}_{k-1,t}^{avH}}{\tilde{\boldsymbol{w}}_{k-1,t}^{avH}\, \tilde{\boldsymbol{s}}(\theta_0)}\right) \tilde{Z}_{kt}\right] \tag{36}$$

where $\tilde{Z}_{kt} = [\tilde{\boldsymbol{z}}_{kt} | \tilde{\boldsymbol{z}}_{k+1,t}]$. The latter simply means that

$$\begin{aligned} \tilde{\boldsymbol{w}}_{kt}^{avH}\, \tilde{\boldsymbol{z}}_{kt} &= \tilde{\boldsymbol{w}}_{k-1,t}^{avH}\, \tilde{\boldsymbol{z}}_{kt} \\ \tilde{\boldsymbol{w}}_{kt}^{avH}\, \tilde{\boldsymbol{z}}_{k+1,t} &= \tilde{\boldsymbol{w}}_{k-1,t}^{avH}\, \tilde{\boldsymbol{z}}_{k+1,t}\,. \end{aligned} \tag{37}$$

The generalization of these three equations for arbitrary κ is obvious.

Note that the hot-clutter "quasi-stationarity" over the $(\kappa+1)$ consecutive repetition periods simply means that the signal eigen-subspace dimension of the resulting averaged covariance matrix should still be less than the total number of degrees of freedom in the STAP filter (MQ). Even when the nonstationarity is significant, proper hot-clutter rejection can be achieved with this averaging provided

$$(\kappa+1)\,[P\,(L+Q-1)] < MQ\,. \tag{38}$$

Recall from (13) that $P(L+Q-1)$ is the rank (signal eigen-subspace dimension) of the "intra-sweep" spatio-temporal hot-clutter-only covariance matrix. Obviously the number of taps Q which guarantees this condition is

$$Q > \frac{(\kappa+1)\,P(L-1)}{M-(\kappa+1)\,P} \tag{39}$$

with the additional necessary condition

$$M > (\kappa+1)\,P\,. \tag{40}$$

To summarize, using the stated hot- and cold-clutter models and operational routines, the above conditions specify the proper choice of purely spatial (M) and total (MQ) degrees of freedom which guarantee high hot-clutter rejectability under almost arbitrary nonstationarity of the hot clutter.

Naturally, the above approach may also be applied to CW OTHR provided there is access to some hot-clutter-only range cells within each PRI.

4. Operational Approach: Finite Sample Size Considerations

The final step towards a truly operational routine is the replacement of the true hot-clutter covariance matrix $\tilde{R}_k^{x\eta}$ by its sample estimate $\hat{\tilde{R}}_k^{x\eta}$. We do this by averaging over all range cells that are free of cold-clutter contamination, for each PRI. For HF OTHR, the size of the hot-clutter training sample used to form $\hat{\tilde{R}}_k^{x\eta}$ is a serious issue. This motivates our investigation into means of reducing the length of the training sequence necessary for hot-clutter cancellation.

One significant contribution has already been made by (14), where the minimum number of taps Q_{min} is given in terms of M, L and P.

According to the famous result of Mallet, Reed and Brennan [16], in order to obtain an average 3 dB loss in SNR compared with the optimum, the number of independent samples T_0 used for estimation of some MQ-variate covariance matrix is

$$T_0 \gtrsim 2MQ\,. \tag{41}$$

Apart from being too large a number in most cases, this estimate does not leave room for the trade-off between the number of spatial and temporal degrees of freedom.

Less well-known are the results of [17, 18, 19], recently duplicated in [20], which show that by proper diagonal loading:

$$\hat{\tilde{R}}_k^{x\eta} = \beta I_{MQ} + \sum_{t=1}^{T_0} (\tilde{x}_{kt} + \tilde{\eta}_{kt})\,(\tilde{x}_{kt} + \tilde{\eta}_{kt})^H \qquad \text{for} \quad \beta \gtrsim \sigma_{\eta}^2 \tag{42}$$

the number of snapshots T_0 sufficient for 3 dB losses may be reduced to

$$T_0 \gtrsim 2\,\text{rank}\;\tilde{R}_k^{x}\,. \tag{43}$$

Recall that the rank of $\tilde{R}_k^{x}$ is equal to the signal eigen-subspace dimension of $\tilde{R}_k^{x\eta}$. Where $\tilde{R}_k^{x\eta}$ is not averaged over adjacent PRIs, this dimension is defined by (13) and (16), *ie.*

$$\text{rank}\;\tilde{R}_k^{x\eta} \leq P(L+Q-1)\,. \tag{44}$$

This firstly means that the "blind zone" can be dramatically reduced (compared with using $T_0 \gtrsim 2MQ$). Secondly, this is analytical evidence for the conclusion made in [21]. Indeed, according to (43) and (44), in order to decrease the 'blind zone', the number of spatial degrees of freedom M should be maximized, followed by the corresponding reduction in temporal degrees of freedom Q.

According to (35) and (42), the operational estimate

$$\hat{\tilde{R}}_k^{av} = \frac{1}{3}\left(\hat{\tilde{R}}_k^{\varkappa\eta} + \hat{\tilde{R}}_{k+1}^{\varkappa\eta} + \hat{\tilde{R}}_{k+2}^{\varkappa\eta}\right) \tag{45}$$

involves $3T_0$ training samples in total. Thus averaging over the (slightly) nonstationary hot-clutter training samples belonging to three consecutive PRIs reduces the random errors for this estimate. Of course, the maximum reduction is obtained when the actual nonstationarity could be ignored:

$$\tilde{R}_k^{\varkappa\eta} \simeq \tilde{R}_{k+1}^{\varkappa\eta} \simeq \tilde{R}_{k+2}^{\varkappa\eta}. \tag{46}$$

Under such extreme circumstances, the total number of necessary training samples ($T_0 = 36$) could even be distributed over these three PRIs.

When there is significant nonstationarity, however, there will be some optimal trade-off in the number of PRIs involved, given that the sample volume T_0 is fixed for each PRI. Indeed by increasing the number of PRIs involved in averaging (K) we increase the signal subspace dimension of the true covariance matrix

$$\tilde{R}_k^{av} = \frac{1}{K+1}\sum_{j=0}^{K}\tilde{R}_{k+j}^{\varkappa\eta}. \tag{47}$$

On the other hand, we somewhat decrease the random error by use of the estimate

$$\hat{\tilde{R}}_k^{av} = \frac{1}{K+1}\sum_{j=1}^{K}\hat{\tilde{R}}_{k+j}^{\varkappa\eta}. \tag{48}$$

Clearly the optimum number K is not identical to the minimum number.

Therefore with simulations that involve the true covariance matrices, we expect covariance matrix averaging to introduce some extra losses in hot-clutter rejectability compared with the ideal case of using $\tilde{R}_k^{\varkappa\eta}$. On the other hand, the fully operational routine using a finite training sample volume per PRI gains in the reduction of stochastic errors due to the averaging process.

The curves labeled q_{OSC} and $\tilde{w}_{OSC}$ in Figs. 1, 2 and 3 demonstrate the efficiency of the fully operational routine, involving a loaded sample covariance matrix, (42) and (45) and simulated data [15]. Comparing the output Doppler spectra obtained for range cells with and without targets, we see that the operational SC STAP routine achieves both highly efficient target detection and subclutter visibility protection. The curve in Fig. 1 indicates the signal-to-hot-clutter ratio for the operational filter across all 256 PRIs. While the 36 training samples are not strictly independent (due to multimode propagation), additional stochastic losses are negligible.

These results show that the operational SC STAP approach can deliver remarkably good performance. Since each range bin is processed by an individual fast-time STAP filter, the cost of such performance is a higher computational load. However for HF OTHR applications at least, where the number of range cells is not large and the Nyquist rate f_t is measured in dozens of kHz, this load is reasonable.

5. SC STAP Algorithm: Efficiency Analysis by Real-Data Processing

The most important remaining question to consider is the adequacy of the scalar low-order AR model which is applied to real cold clutter. This question has been partly discussed in [3]. Here we refer to some new real HF OTHR clutter data to illustrate the ability of the proposed SC STAP algorithm to retain the initial subclutter visibility.

The first set of experimental data was collected by the Jindalee facility, located in Alice Springs, Australia [22]. Typical sky-wave sea-scattered signals have been collected by the 32-channel receiver in its ship-detection mode, without noticeable jamming. The interference signals were recorded separately, when the system operated in receive-only mode. This experimental setup allowed us to compare in [15] the initial and "stabilized" cold-clutter spectra with one, two and four constraints.

While a single stochastic constraint is inadequate, with subclutter visibility degrading up to about 15 dB, two and four constraints gave output spectra that are practically identical to the CBF spectra. This provides a justification of our use of the simple AR cold-clutter model for sky-wave OTHR applications.

For surface-wave radars, the sea-clutter is even closer to its theoretical model, introduced in [23]. We present one example from the data set collected by the 12-channel pulse-waveform SW OTHR facility, operating with a PRF of 10 Hz and CPI of 100 seconds. Figs. 4 and 5 together illustrate (a) the standard CBF spectrum corresponding to the filter $\tilde{w}_{CBF}$, and the output spectra obtained for (b) globally averaged STAP (constant for all PRIs) $\tilde{w}_{\overline{STAP}}$, (c) SC STAP with two constraints $\tilde{w}_{SC}$, and (d) unconstrained STAP $\tilde{w}_{STAP}$. The first three spectra are indistinguishable, whereas the unconstrained STAP filter fluctuations degrade subclutter visibility significantly. Note that the CBF subclutter visibility (rather poor in this case) is retained without any noticeable broadening of the narrow-band Doppler components (Bragg lines).

These results demonstrate that, despite the complexity of global models that properly describe real HF sea-clutter, we may apply simplistic models locally without major degradation.

6. Summary and Conclusions

We have identified the similarity between HF OTH radars, with respect to the problem of multimode-interference (hot-clutter) rejection utilizing STAP. The problem of nonstationary hot-clutter cancellation via fast-time STAP has been formulated, mainly relying upon recently investigated properties of HF signals propagating through perturbed ionospheric regions.

It has been demonstrated that the standard fast-time STAP algorithms are inappropriate for the removal of nonstationary hot clutter when the backscattered signal (cold clutter) properties must be preserved in some way. Fast-time (intra-PRI) STAP filters that vary from PRI to PRI in an unconstrained fashion cause a severe degradation in the cold-clutter Doppler spectral properties (namely, subclutter visibility). On the other hand, the application of time-independent STAP algorithms, for which the hot-clutter spatio-temporal covariance matrix is averaged over a relatively long CPI, severely degrades the hot-clutter rejectability.

The only previously known approach that can theoretically perform simultaneous hot- and cold-clutter rejection is the "uniform STAP". This has a problem size defined by MNQ, where M is the number of antenna receivers, N is the number of PRIs within each CPI, and Q is the number of fast-time taps. For all HF OTHR applications, where typical values are $M = 16$ to 32 and $N = 128$ to 256, this approach is practically useless, simply because of the lack of sufficient training samples needed to adapt the system.

With the goal of overcoming these limitations of the standard approach, this study has investigated the theoretical existence of slow-time-varying fast-time spatio-temporal filters that can provide high hot-clutter rejectability and stationarity of the hot-clutter scalar output signal. We have demonstrated that for a particular multivariate scalar low-order AR model of the cold clutter, data-dependent ("stochastic") constraints can retain the stationarity of the cold-clutter scalar output.

Operational routines that implement the main principles of the proposed theoretic SC STAP were then introduced (in the context of HF OTHR applications). Here the *a priori* known distinctions between the hot- and cold-clutter distributions in range are exploited. More specifically, the ranges that are always free of cold clutter (in pulse-waveform radar systems) are utilized for accurate hot-clutter covariance matrix estimation. The efficiency of the SC STAP approach has been demonstrated by simulations, conducted for typical HF OTHR scenarios.

These simulations have demonstrated the high efficiency of the SC STAP algorithm, both in hot-clutter rejection and in cold-clutter post-processing.

Finally, real sky-wave and surface-wave OTHR sea-scattered data has been processed in order to show that a simple AR model of the cold clutter can be used locally over a small number of adjacent PRIs in forming stochastic constraints, despite the fact that real cold clutter is globally far from being properly described by this model.

Thus, for typical HF OTHR applications the proposed SC STAP method is verified. The performance achieved comes at a considerable computation cost: each range cell should be processed by an individual STAP filter that should be updated each PRI, ideally. Obviously, each finger-beam requires an individual set of SC STAP filters. Nevertheless, for HF OTHR with a modest number of range cells and a comparatively low bandwidth, this computational load is reasonable.

References

[1] A.A. Kolosov, *Over-the-horizon radar*, Artech House, Boston, 1987, English translation by W.F. Barton.

[2] T.M. Blake, "Ship detection and tracking using high frequency surface wave radar," in *Proc. 7th Int. Conf. on HF Radio Systems and Techniques*, 1997, pp. 291–295.

[3] Y.I. Abramovich, F.F. Yevstratov, and V.N. Mikhaylyukov, "Experimental investigation of efficiency of adaptive spatial unpremeditated noise compensation in HF radars for remote sea surface diagnostics," *Soviet Journal of Communication Technology and Electronics*, vol. 38 (10), pp. 112–118, 1993, English translation of *Radioteknika i Elektronika*.

[4] R. Fante and J.A. Torres, "Cancellation of diffuse jammer multipath by an airborne adaptive radar," *IEEE Trans. Aero. Elect. Sys.*, vol. 31 (2), pp. 805–820, 1995.

[5] D. Marshall and R. Gavel, "Simultaneous mitigation of multipath jamming and ground clutter," in *Proc. Adaptive Sensor Array Processing Workshop*, MIT Lincoln Laboratory, 1996, vol. 1, pp. 193–239.

[6] Y.I. Abramovich, V.N. Mikhaylyukov, and I.P. Malyavin, "Stabilisation of the autoregressive characteristics of spatial clutters in the case of nonstationary spatial filtering," *Soviet Journal of Communication Technology and Electronics*, vol. 37 (2), pp. 10–19, 1992, English translation of *Radioteknika i Elektronika*.

[7] Y.I. Abramovich, A.Y. Gorokhov, V.N. Mikhaylyukov, and I.P. Malyavin, "Exterior noise adaptive rejection for OTH radar implementations," in *Proc. ICASSP-94*, Adelaide, 1994, vol. 6, pp. 105–107.

[8] Y.I. Abramovich and A.Y. Gorokhov, "Adaptive OTHR signal extraction under nonstationary ionospheric propagation conditions," in *Proc. RADAR-94*, Paris, 1994, pp. 420–425.

[9] L.J. Griffiths, "Linear constraints in hot clutter cancellation," in *Proc. ICASSP-96*, Ātlanta, 1996, vol. 2, pp. 1181–1184.

[10] Y.I. Abramovich and S.A. Zaytsev, "One interpretation of the optimum algorithm for the detection of a signal masked by distributed interfering reflections," *Radio Eng. Electron. Phys.*, vol. 24 (5), pp. 25–32, 1979.

[11] Y.I. Abramovich and V.G. Kachur, "Characteristics of adaptive spatial clutter rejection," *Radio Eng. Electron. Phys.*, vol. 28 (9), pp. 57–64, 1983.

[12] A.Y. Gorokhov and P. Loubaton, "Subspace based techniques for blind separation of convolutive mixtures with temporally correlated sources," *IEEE Trans. on Circuits and Systems – I*, vol. 44 (9), pp. 813–820, 1997.

[13] S. Haykin, *Adaptive Filter Theory*, Prentice Hall, New Jersey, 1996, 3rd edition.

[14] K. Abed-Meraïm *et al.*, "Prediction error methods for time domain blind identification of multichannel FIR filters," in *Proc. ICASSP-95*, Detroit, 1995, pp. 1968–1971.

[15] Y.I. Abramovich, N.K. Spencer, S.J. Anderson, and A.Y. Gorokhov, "Stochastic-constraints method in nonstationary hot-clutter cancellation — Part I: Fundamentals and supervised training applications," *IEEE Trans. Aero. Elect. Sys.*, vol. 34 (4), pp. 1271–1292, 1998.

[16] J.D. Mallet, I.S. Reed, and L.E. Brennan, "Rapid convergence rate in adaptive arrays," *IEEE Trans. Aero. Elect. Sys.*, vol. 10 (6), pp. 853–863, 1974.

[17] Y.I. Abramovich, "A controlled method for adaptive optimization of filters using the criterion of maximum SNR," *Radio Eng. Electron. Phys.*, vol. 26 (3), pp. 87–95, 1981.

[18] Y.I. Abramovich and A.I. Nevrev, "An analysis of effectiveness of adaptive maximization of the signal-to-noise ratio which utilizes the inversion of the estimated correlation matrix," *Radio Eng. Electron. Phys.*, vol. 26 (12), pp. 67–74, 1981.

[19] O.P. Cheremisin, "Efficiency of adaptive algorithms with regularised sample covariance matrix," *Radio Eng. Electron. Phys.*, vol. 27 (10), pp. 69–77, 1982.

[20] C.H. Gierull, "Performance analysis of fast projections of the Hung–Turner type for adaptive beamforming," *Signal Processing (Eurosip special issue on Subspace Methods for Detection and Estimation, Part I)*, vol. 50, pp. 17–28, 1996.

[21] S.M. Kogon, D.B. Williams, and E.J. Holder, "Beamspace techniques for hot clutter cancellation," in *Proc. ICASSP-96*, Atlanta, 1996, vol. 2, pp. 1177–1180.

[22] S.J. Anderson, S.E. Godfrey, and S.M. Vright, "On model identification for distortion correction of OTH radar," in *Proc. ICASSP-94*, Adelaide, 1994, vol. 6, pp. 129–132.

[23] D.E. Barrick and J.B. Snider, "The statistics of HF sea-echo Doppler spectra," *IEEE Trans. Ant. Prop.*, vol. 25 (1), pp. 19–28, 1977.

	Mode 1	Mode 2	Mode 3	Mode 4
jammer direction-of-arrival ($\theta^{1\ell}$) (degrees)	0.5	20.5	39.3	44.9
hot-clutter-to-noise ratio (HCNR) (dB)	30	25	20	35
temporal correlation coefficient ($\rho^{1\ell}$)	1.00	0.90	0.88	0.91
spatial correlation coefficient ($\zeta^{1\ell}$)	1.00	0.91	0.90	0.90

Table 1: Hot clutter simulation parameters.

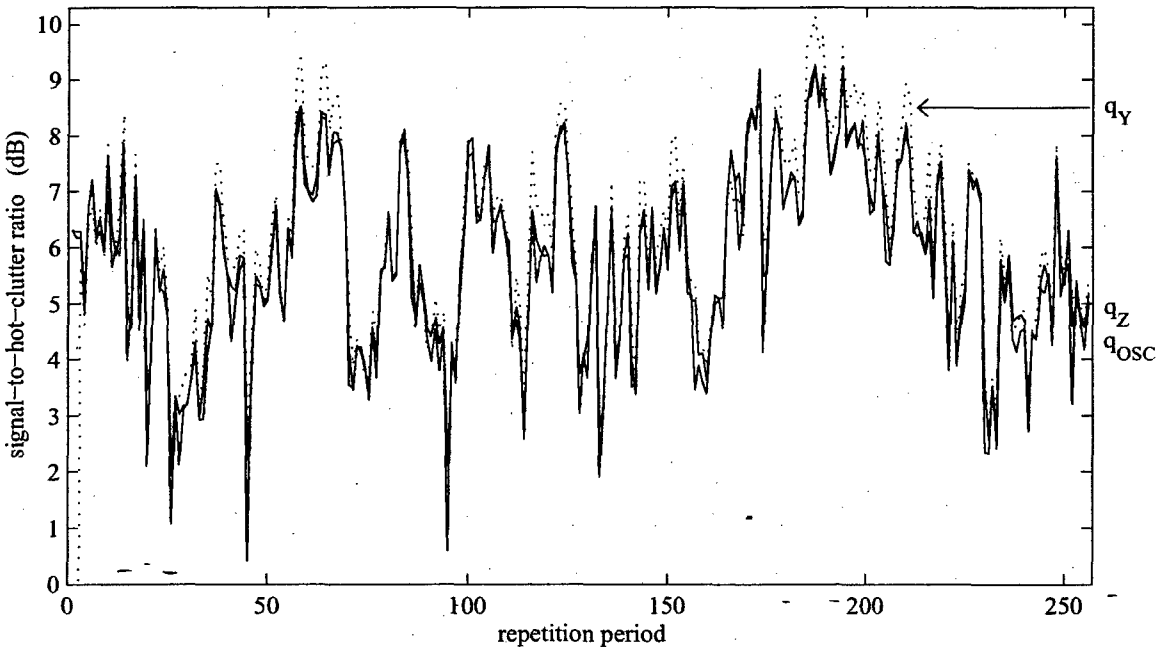

Figure 1: Several stages in the SHRC analysis of the SC STAP operational routine.

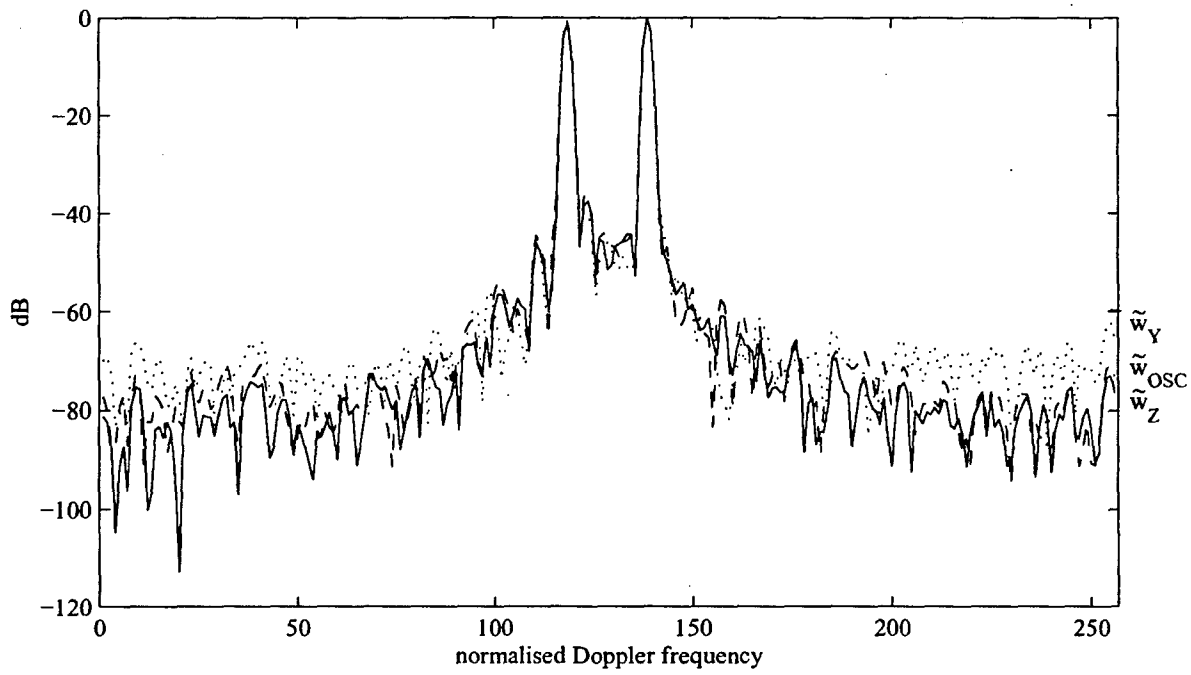

Figure 2: Several stages in the analysis of the weighted FFT Doppler spectra for a range cell containing only cold clutter.

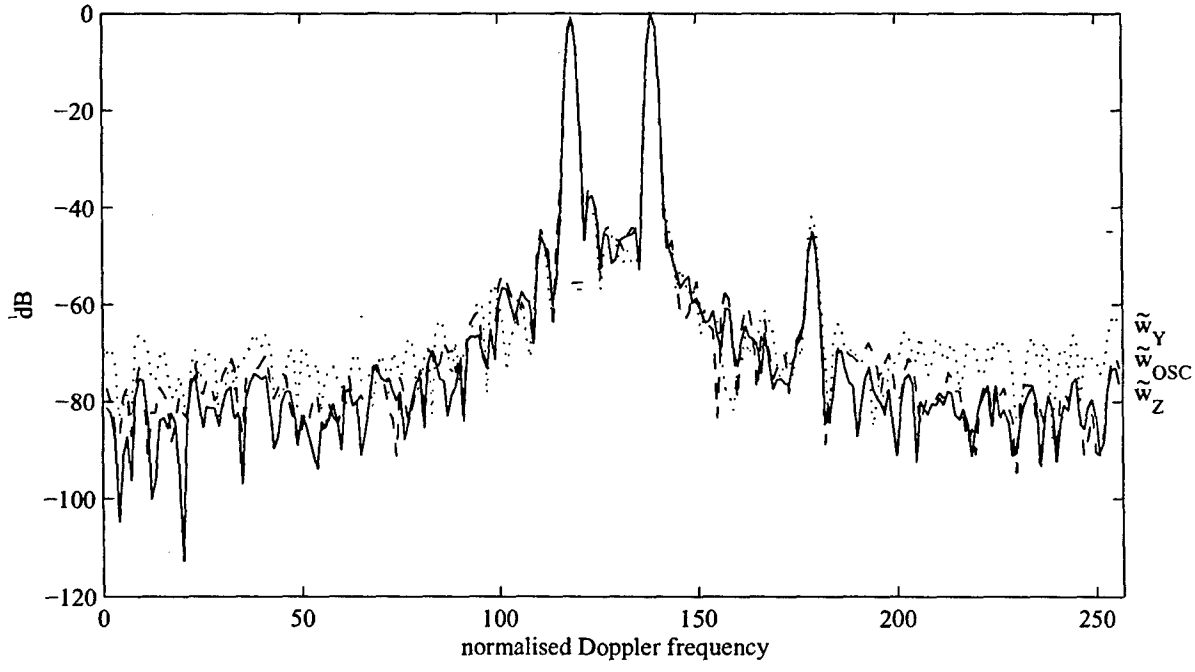

Figure 3: Identical simulation parameters as for Fig. 2, but with a target present.

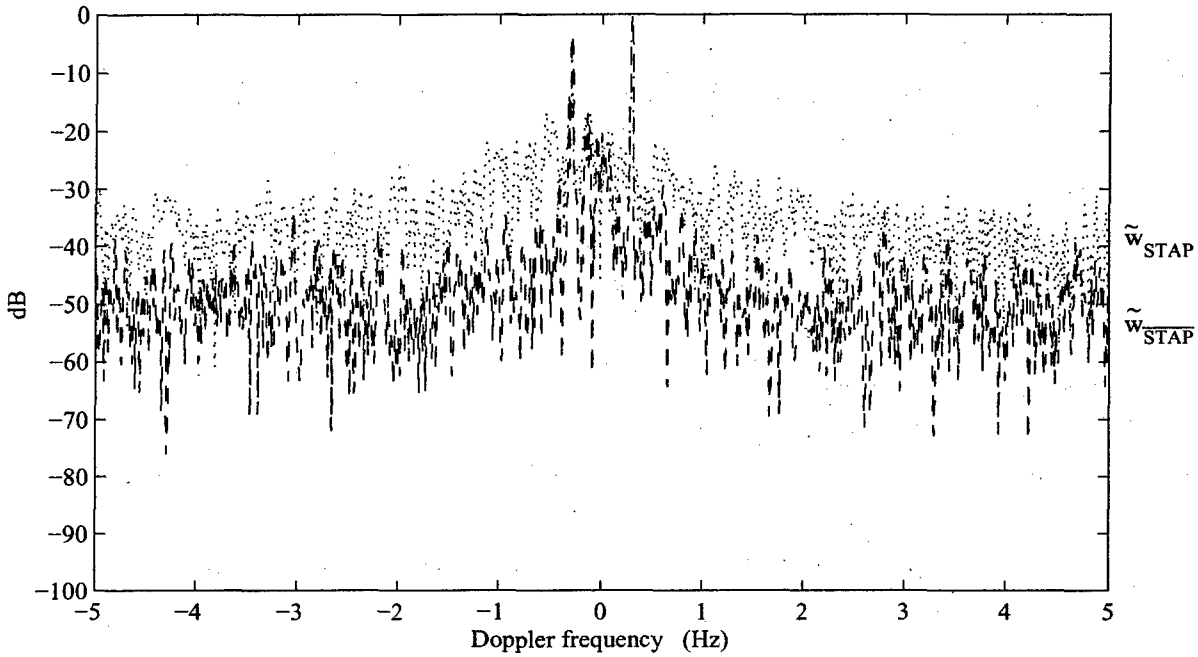

Figure 4: Real SW Doppler spectra processed by two different filters.

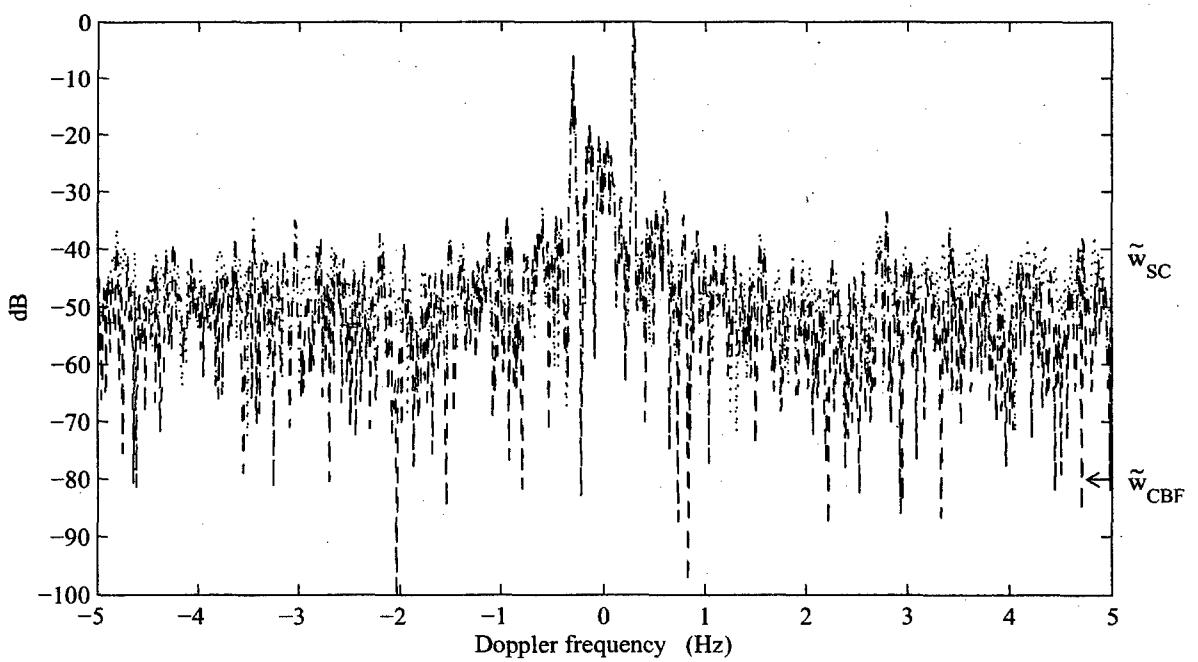

Figure 5: Identical real-data as in Fig. 4, processed by two further filters.

List of Major Notation

$I_n \in \mathcal{R}^{n\times n}$ = identity matrix

$\delta(m,n)$ = generalized Kronecker delta function

$\boldsymbol{e}_n \in \mathcal{R}^{n\times 1} = [1,0,\ldots,0]^T$

N = number of transmitted pulses or sweeps = number of repetition periods

$k = 1,\ldots,N$ = slow-time index variable

f_r = pulse repetition frequency (pulses per second)

M = number of antenna array sensors

f_t = Nyquist rate at which receiver outputs are sampled (samples per second)

T = samples per pulse repetition interval (PRI)

$t = 1,\ldots,T$ = fast-time index variable

Q = number of fast-time taps

$\boldsymbol{z}_{kt} \in \mathcal{C}^{M\times 1}$ = antenna array snapshot for the k^{th} repetition period and the t^{th} range bin

$\boldsymbol{s}_{kt} \in \mathcal{C}^{M\times 1}$ = target signal

$\boldsymbol{y}_{kt} \in \mathcal{C}^{M\times 1}$ = cold clutter

$\boldsymbol{x}_{kt} \in \mathcal{C}^{M\times 1}$ = hot clutter

$\boldsymbol{\eta}_{kt} \in \mathcal{C}^{M\times 1}$ = additive white noise

$\sigma^2_{\boldsymbol{\eta}} \in \mathcal{R}$ = power of additive white noise

θ_0 = target-signal DOA (degrees)

$\boldsymbol{s}(\theta_0) \in \mathcal{C}^{M\times 1}$ = antenna array manifold ("steering") vector for the look direction θ_0

$R_k^{\boldsymbol{y}} \in \mathcal{H}^{M\times M}$ = cold-clutter spatial covariance matrix at the slow-time lag k

$R_0^{\boldsymbol{y}} \in \mathcal{H}^{M\times M}$ = standard cold-clutter spatial covariance matrix

P = number of external interference (jamming) signals (index variable $p = 1,\ldots,P$)

$g_{kt}^{(p)} \in \mathcal{C}$ = complex waveform representing the p^{th} external interferer (jammer)

L = number of propagating paths for the jammers (index variable $\ell = 1,\ldots,L$)

$H_{k\ell} \in \mathcal{C}^{M\times P}$ = instantaneous total impulse response

$\boldsymbol{g}_{kt} \in \mathcal{C}^{P\times 1}$ = complex waveform vector representing all jammer signals

$\sigma^2_{\boldsymbol{x}_p} \in \mathcal{R}$ = the p^{th} jamming signal power

$\tilde{\boldsymbol{z}}_{kt} \in \mathcal{C}^{MQ\times 1}$ = Q-stacked antenna array snapshot

$\tilde{\boldsymbol{s}}_{kt} \in \mathcal{C}^{MQ\times 1}$ = Q-stacked target signal snapshot

$\tilde{\boldsymbol{y}}_{kt} \in \mathcal{C}^{MQ\times 1}$ = Q-stacked cold clutter snapshot

$\tilde{\boldsymbol{x}}_{kt} \in \mathcal{C}^{MQ\times 1}$ = Q-stacked hot clutter snapshot

$\tilde{\boldsymbol{w}}_{kt} \in \mathcal{C}^{MQ\times 1}$ = Q-stacked STAP filter

$\tilde{H}_{k\ell} \in \mathcal{C}^{MQ\times P(L+Q-1)}$ = Q-stacked instantaneous total impulse response matrix

$\tilde{\boldsymbol{g}}_{kt} \in \mathcal{C}^{P(L+Q-1)\times 1}$ = Q-stacked jammer waveform vector

$\tilde{R}_k^{\boldsymbol{x}} \in \mathcal{H}^{MQ\times MQ}$ = Q-blocked noise-free hot-clutter spatio-temporal covariance matrix

$z_{kt} \in \mathcal{C}$ = output from the Q-stacked STAP filter applied to the Q-stacked array snapshot

$s_{kt} \in \mathcal{C}$ = output from the Q-stacked STAP filter applied to the Q-stacked target signal

$y_{kt} \in \mathcal{C}$ = output from the Q-stacked STAP filter applied to the Q-stacked cold clutter

$x_{kt} \in \mathcal{C}$ = output from the Q-stacked STAP filter applied to the Q-stacked hot clutter

q = number of linear constraints imposed on the Q-stacked STAP filter

$\tilde{A}_q \in \mathcal{C}^{MQ\times q}$ = Q-stacked general deterministic linear constraint matrix

κ = order of the cold-clutter AR model

$B_j \in \mathcal{C}^{M\times M}$ = cold-clutter AR model parameters = Yule-Walker solutions ($j = 1, \ldots, \kappa$)

$\boldsymbol{\xi}_{kt} \in \mathcal{C}^{M\times 1}$ = innovative noise in AR model

$R_k^{\boldsymbol{\xi}} \in \mathcal{H}^{M\times M}$ = innovative noise spatial covariance matrix

$\tilde{B}_j \in \mathcal{C}^{MQ\times MQ}$ = Q-blocked cold-clutter AR model parameters

$\tilde{\boldsymbol{\xi}}_{kt} \in \mathcal{C}^{MQ\times 1}$ = Q-stacked innovative noise in AR model

$\tilde{R}_k^{\boldsymbol{\xi}} \in \mathcal{H}^{MQ\times MQ}$ = Q-blocked innovative noise spatial covariance matrix

$\tilde{\boldsymbol{w}}_0 \in \mathcal{C}^{MQ\times 1}$ = any given constant Q-stacked STAP filter

$y_{kt}^{(0)} \in \mathcal{C}$ = cold-clutter scalar output for the above filter

$\tilde{R}_k^{\boldsymbol{x}\boldsymbol{\eta}} \in \mathcal{H}^{MQ\times MQ}$ = Q-blocked hot-clutter-plus-noise covariance matrix

$\tilde{\boldsymbol{s}}(\theta_0) \in \mathcal{C}^{\ Q\ 1}$ = Q-stacked steering vector for the look direction θ_0

$\tilde{Y}_{kt} \in \mathcal{C}^{MQ\times\kappa}$ = Q-stacked stochastic-constraints matrix

$\tilde{A}_{kt} \in \mathcal{C}^{MQ\times(\kappa+q)}$ = ideal augmented linear stochastic constraints matrix (cold clutter only)

$b_j \in \mathcal{C}$ = cold-clutter (simplified scalar) AR model parameters

$r_j \in \mathcal{C}$ = correlation coefficients of the (simplified scalar) cold-clutter process

$\sigma_{\boldsymbol{\xi}}^2 \in \mathcal{R}$ = power of the innovative noise in the (simplified scalar) AR model

$\tilde{\boldsymbol{w}}_{kt}^{\boldsymbol{qw}} \in \mathcal{C}^{MQ\times 1}$ = stochastically unconstrained STAP filter (hot-clutter-plus-noise only)

$\tilde{R}_k^{\boldsymbol{qw}} \in \mathcal{C}^{MQ\times MQ}$ = moving-window average of hot-clutter-plus-noise-only samples

$\tilde{A}_{kt}^{\boldsymbol{z}} \in \mathcal{C}^{MQ\times(\kappa+q)}$ = operational augmented linear stochastic constraints matrix

J = order of the generalized Watterson model for ionospherically propagated hot clutter

$\rho^{p\ell}$ = temporal correlation coefficient

$\varsigma^{p\ell}$ = spatial correlation coefficient

K = number of PRIs involved in averaging